Green's function theory of the two-dimensional antiferromagnetic Heisenberg model with local magnetic impurities

2000 J. Phys.: Condens. Matter 12 5275

(http://iopscience.iop.org/0953-8984/12/24/316)

J. Phys.: Condens. Matter **12** (2000) 5275–5285. Printed in the UK PII: S0953-8984(00)10450-3

Green's function theory of the two-dimensional antiferromagnetic Heisenberg model with local magnetic impurities

Yun Song†‡, H Q Lin† and A W Sandvik§

† Department of Physics, The Chinese University of Hong Kong, Shatin, NT, Hong Kong, China
‡ Department of Physics, Beijing Normal University, Beijing, 100875, China‖
§ Department of Physics, University of Illinois at Urbana-Champaign, Urbana, IL 61801, USA

Received 20 December 1999, in final form 4 April 2000

Abstract. Two-dimensional spin-1/2 Heisenberg antiferromagnets with nonmagnetic or ferromagnetic impurities are studied using an improved Green's function theory and quantum Monte Carlo simulations over the whole temperature region. The antiferromagnetic spin correlation functions at the bonds closest to the impurities are found to be enhanced in both the nonmagnetic and ferromagnetic impurity cases at all temperatures. For the nonmagnetic impurity case, our numerical results for spin correlation functions and ground-state energies agree with those from previous Monte Carlo simulations. For the ferromagnetic impurity case, we found that the spin-wave excitations are strongly influenced by the impurities. Discrete local modes emerge above the continuous spin-wave excitations. The effects of the distance between two ferromagnetic impurities on the local modes are also investigated.

1. Introduction

Impurity effects in cuprate superconductors have attracted much attention from researchers attempting to achieve an understanding of the role of electron correlations in high-temperature superconductivity [1, 2]. The extreme limit of static holes or magnetic defects is also believed to have physical relevance to this issue. Accordingly, there have been many experiments [3–5] addressing the problem of impurity states in the antiferromagnetic (AF) parent compounds of high-T_C superconductors. The most representative case is that of nonmagnetic Zn substitution for Cu in the CuO_2 plane of $La_2Cu_{1-x}Zn_xO_4$.

The two-dimensional (2D) site-random (SR) Heisenberg model can be used to describe the CuO_2 plane with a random distribution of static holes or magnetic defects. There have been many theoretical studies carried out to investigate the magnetic properties of the 2D SR Heisenberg model. Examples include work based on the linear spin-wave (LSW) theory [6, 7] and the coherent potential approximation [8, 9], exact-diagonalization studies [10], and quantum Monte Carlo (QMC) simulations [11–13]. However, there are still discrepancies among the results from analytical theories and computer simulations.

In 2D, the Heisenberg model does not exhibit long-range order (LRO) for any spin at finite temperature [14]. There is, however, solid numerical evidence that the ground state of the spin-1/2 AF Heisenberg on a square lattice is characterized by AF LRO [15] (for $S > 1/2$, the existence of long-range order has been proven rigorously [16]). A second-order

‖ Mailing address.

0953-8984/00/245275+11$30.00

Green's function (SOGF) theory [17, 18] has been quite successfully used in studying the low-dimensional Heisenberg model over the whole temperature region. For finite temperatures, Shimahara and Takada [18] found that the low-lying excitation of the 2D AF Heisenberg model is a kind of spin wave propagating against a background of short-range AF order, and their spin-wave spectrum depends only on the short-range spin correlation functions. In the ground state, the SOGF theory predicts the existence of AF LRO dual to Bose condensation, and the spin-wave spectrum is analogous to that of the LSW theory [20]. It has been proved that [17, 18], at high temperature, this theory reproduces correctly the results obtained by the high-temperature expansion method [21]. On the other hand, the results at low temperature are similar to those from the modified spin-wave theory [22]. Results from SOGF theory are in qualitative agreement with numerical results [23, 24] over the whole temperature region.

The SOGF theory has been successfully applied to many low-dimensional homogeneous systems [17, 18, 25, 26]. In an earlier work [27], we introduced an improved decoupling approximation and examined our new method by studying the 2D Heisenberg model with broken bonds. It has been shown that the improved SOGF theory [27] is applicable to spin systems with spatial inhomogeneity introduced by the local defects. In this paper, we have applied the improved SOGF theory to study the 2D SR Heisenberg model. We have also performed quantum Monte Carlo simulations for comparison.

The paper is organized as follows. In section 2 we introduce the SR Heisenberg model and the improved SOGF theory. Our numerical results for the 2D SR Heisenberg model with nonmagnetic and ferromagnetic impurities are presented in section 3 and section 4, respectively. Finally, we conclude with our findings in section 5.

2. The SR Heisenberg model and improved SOGF theory

Consider the SR spin system described by the following Hamiltonian:

$$H = \sum_{\langle ij \rangle} J_{ij} n_i n_j \left\{ \frac{1}{2}(S_i^+ S_j^- + S_i^- S_j^+) + S_i^z S_j^z \right\} \tag{1}$$

where $\langle ij \rangle$ denotes a sum over nearest-neighbour (NN) bonds (there are a total of $2N$ bonds for an N-site 2D lattice), n_i is a random variable taking the value of 1 or 0 according to whether or not the site i is occupied by a magnetic atom, and J_{ij} is the exchange interaction between sites i and j.

We introduce the spin Green's functions G via

$$G(i-j, t-t') = -\mathrm{i}\theta(t-t')\langle [n_i S_i^z(t); n_j S_j^z(t')] \rangle \equiv \langle\langle \widetilde{S}_i^z(t); \widetilde{S}_j^z(t') \rangle\rangle \tag{2}$$

where $\theta(t)$ is the step function, $\widetilde{S}_i^z = n_i S_i^z$, and $\langle \cdots \rangle$ defines the ensemble average. Since the Fourier transform of the double-time Green's function satisfies the following equation:

$$\omega \langle\langle A; B \rangle\rangle_\omega = \frac{1}{2\pi} \langle [A, B] \rangle_\omega + \langle\langle [A, H]; B \rangle\rangle_\omega \tag{3}$$

the equation of motion of the spin Green's function G can be evaluated as

$$\omega G(i-j, \omega) = \sum_\eta J_{i,i+\eta} n_i \langle\langle \widetilde{S}_i^+ \widetilde{S}_{i+\eta}^- - \widetilde{S}_{i+\eta}^+ \widetilde{S}_i^-; \widetilde{S}_j^z \rangle\rangle_\omega \tag{4}$$

with $\eta = \hat{x}, \hat{y}$, $\widetilde{S}_i^+ = n_i S_i^+$, and $\widetilde{S}_i^- = n_i S_i^-$. Going a step further, we establish the equation of

motion of the higher-order spin Green's function:

$$\begin{aligned}\omega\langle\langle \widetilde{S}_i^+\widetilde{S}_{i+\eta}^- - \widetilde{S}_{i+\eta}^+\widetilde{S}_i^-;\, \widetilde{S}_j^z\rangle\rangle_\omega &= n_j(\langle \widetilde{S}_i^+\widetilde{S}_{i+\eta}^-\rangle + \langle \widetilde{S}_i^-\widetilde{S}_{i+\eta}^+\rangle)(\delta_{i+\eta,j} - \delta_{i,j}) \\ &+ 2J_{i,i+\eta}n_i n_{i+\eta}\langle\langle n_{i+\eta}\widetilde{S}_i^z - n_i\widetilde{S}_{i+\eta}^z;\, \widetilde{S}_j^z\rangle\rangle_\omega \\ &+ \sum_{\eta'\neq\eta}\langle\langle \Lambda_i(\eta,\eta') - \Lambda_{i+\eta}(-\eta,-\eta');\, \widetilde{S}_j^z\rangle\rangle_\omega \end{aligned} \tag{5}$$

where

$$\Lambda_{i,i+\eta} = 2J_{i,i+\eta'}n_i[(\widetilde{S}_{i+\eta'}^+\widetilde{S}_{i+\eta}^- + \widetilde{S}_{i+\eta'}^-\widetilde{S}_{i+\eta}^+)\widetilde{S}_i^z - (\widetilde{S}_i^+\widetilde{S}_{i+\eta}^- + \widetilde{S}_i^-\widetilde{S}_{i+\eta}^+)\widetilde{S}_{i+\eta'}^z]. \tag{6}$$

As described in reference [27], we use an improved decoupling scheme:

$$\langle\langle S_m^+S_n^-S_i^z;\, S_j^z\rangle\rangle \to \beta_m\langle S_m^+S_n^-\rangle\beta_n\langle\langle S_i^z;\, S_j^z\rangle\rangle \tag{7}$$

and rewrite the equation of motion for the spin Green's function G:

$$\begin{aligned}\omega^2 G(i-j,\omega) = \sum_\eta\Bigg\{ J_{i,i+\eta}n_i\Bigg[& 4n_j C(i,i+\eta)(\delta_{i+\eta,j} - \delta_{i,j}) \\ &+ 2J_{i,i+\eta}n_i n_{i+\eta}\langle\langle n_{i+\eta}\widetilde{S}_i^z - n_i\widetilde{S}_{i+\eta}^z;\, \widetilde{S}_j^z\rangle\rangle \\ &+ \sum_{\eta\neq\eta'}\langle\langle \Pi_i(\eta,\eta') - \Pi_{i+\eta}(-\eta,-\eta');\, \widetilde{S}_j^z\rangle\rangle\Bigg]\Bigg\} \end{aligned} \tag{8}$$

with

$$\begin{aligned}\Pi_i(\eta,\eta') &= 8J_{i,i+\eta'}n_i[\beta_{i+\eta}\beta_{i+\eta'}C(i+\eta,i+\eta')\widetilde{S}_i^z - \beta_{i+\eta}\beta_i C(i,i+\eta)\widetilde{S}_{i+\eta'}^z] \\ C(i,j) &= \frac{1}{2}\langle \widetilde{S}_i^+\widetilde{S}_j^-\rangle = \langle \widetilde{S}_i^z\widetilde{S}_j^z\rangle. \end{aligned} \tag{9}$$

Since lattice translational invariance is not present in the inhomogeneous case, we can only solve the above equations in real space. On a finite lattice, the spin Green's function G can be expressed in a matrix form $\widetilde{G}$, and equation (8) can be rewritten as

$$\omega^2\widetilde{G} - \widetilde{h}\,\widetilde{G} = \widetilde{C} \tag{10}$$

where the matrices $\widetilde{h}$ and $\widetilde{C}$ are determined by the NN, second-NN, and third-NN spin correlation functions. Thus we obtain the self-consistent equations for determining the spin correlation functions and the vertex correction parameters β_i for each site i. Previously, we have compared our results for the 8×8 lattice for the homogeneous case to those for the infinite lattice obtained by Shimahara and Takada [18] and the agreement was good [27]. That is, our numerical calculations can give reasonable estimates for problems in the infinite spin systems that we are interested in.

3. Nonmagnetic impurity case

In this section, we study the local effect of nonmagnetic impurities in 2D Heisenberg antiferromagnets. Our numerical calculations are for the 8×8 lattice with periodic boundary conditions. For this system with only one impurity, our numerical results for the NN correlation functions near the isolated nonmagnetic impurity at temperature $T = 0.05$ (measured in units of J) are displayed in figure 1. We find that the nonmagnetic impurity enhances the NN AF correlation functions for spins close to it; that is, the quantum fluctuation for spins close to the nonmagnetic impurity is reduced. The largest value of the NN correlation function in figure 1 is $C_1 = -0.1155$, which is about 10% higher than that for the NN correlation function, $C_1 = -0.1035$, of the homogeneous 8×8 lattice. Behre and Miyashita [12] have

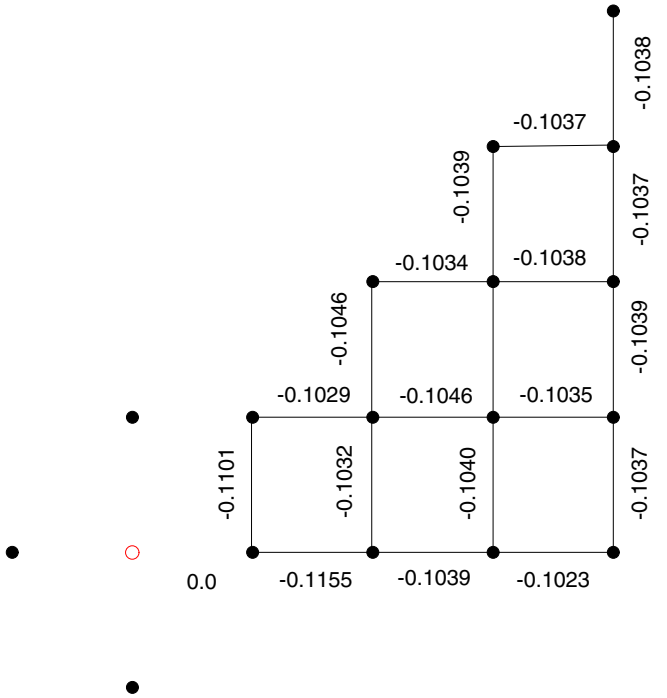

Figure 1. Nearest-neighbour correlation functions for the 8×8 lattice with one nonmagnetic impurity at temperature $T/J = 0.05$. The open circle represents the nonmagnetic impurity.

applied a QMC technique to this model and found that NN correlations which are further away from the impurity are enhanced by more than 4% for the 4×4 lattice at temperature $T = 0.05$. Our results are in agreement with those of QMC simulations [11, 12]. At zero temperature, Bulut *et al* [7] have studied this model using the LSW theory and their results also showed that quantum fluctuation is reduced in the neighbourhood of the static vacancy.

We have investigated the 8×8 lattices with two (the doping density is $n = 0.031\,25$) and four ($n = 0.0625$) nonmagnetic impurities, respectively, by performing configuration averaging over the randomness of the impurity positions. The average spin correlation function $C(r)$ in our calculation is defined as

$$C(r) = \left(\sum_i \overline{\langle S_i^z S_{i+r}^z \rangle}\right) \Big/ N = \left[\sum_i \left(\sum_m \langle S_i^z S_{i+r}^z \rangle_m\right) \Big/ M\right] \Big/ N \tag{11}$$

where M is the number of samples. The distance dependences of the average spin correlation functions $C(r)$ for $n = 0.0625$ and $n = 0$ are shown in figure 2(a). For convenience of comparison, the results of the QMC simulation on the 8×8 lattice [12] are also plotted in figure 2(a). Our results are in fairly good agreement with those from the QMC simulations [11,12]. We found that, as the doping density n increases, the average spin correlation function $C(r)$ decreases. Our numerical results also show that although the quantum fluctuation for spins close to the nonmagnetic impurities is reduced, the average of the quantum fluctuations over the whole lattice is strengthened. The ground-state energies as functions of doping density n are plotted in figure 2(b). It shows that the absolute value of the ground-state energy decreases as the density of nonmagnetic impurities increases, which is in agreement with the results from MC simulations [11, 12].

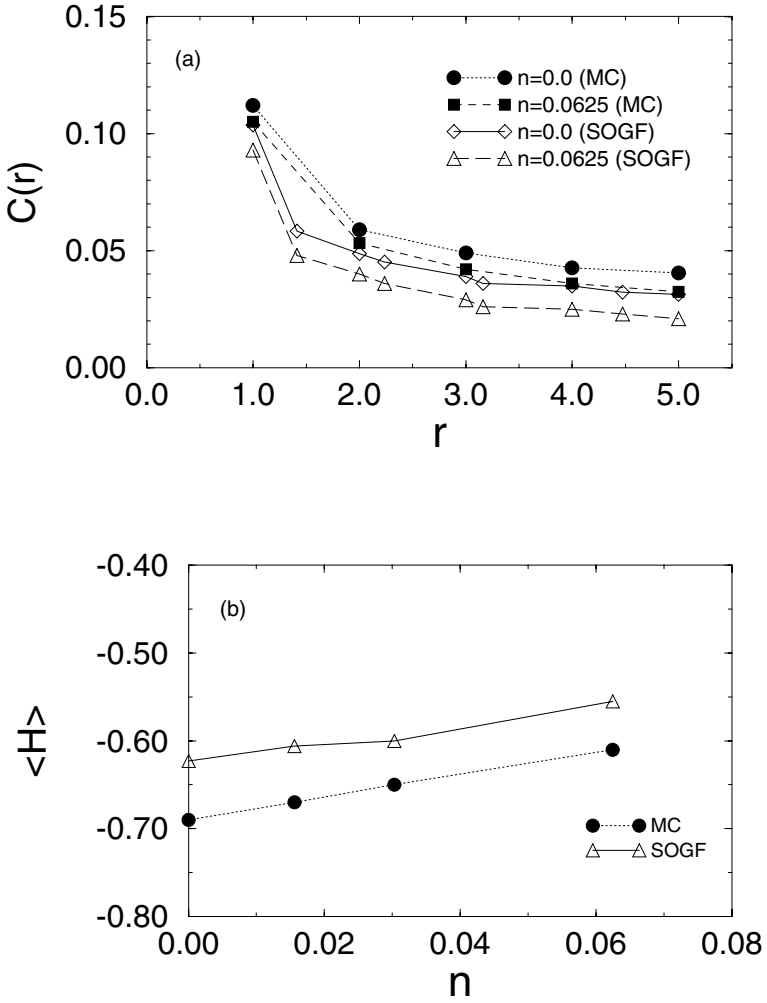

Figure 2. (a) The distance dependence of the average spin correlation function $C(r)$. (b) The average intrinsic energy versus doping density.

4. Ferromagnetic impurity case

In this section, we consider the 2D Heisenberg antiferromagnet with ferromagnetic impurities. This system is a mixture of two kinds of magnetic ion A (antiferromagnetic) and B (ferromagnetic). The integrals for exchange between neighbouring ion pairs are arranged as follows: $+J$ for A–A bonds, $-J_F$ for B–B and A–B bonds. We first set $J_F = J$, and investigate the system with only one impurity with periodic boundary conditions. As an example, we show our numerical results for the NN correlation functions near the isolated impurity at temperature $T = 0.05$ for an 8×8 lattice in figure 3. Our results show that the quantum fluctuation near the ferromagnetic impurity is also reduced, similarly to the case for the nonmagnetic impurity. From figure 3, we obtain that the NN correlation function on the ferromagnetic bond is $C_1 = 0.0825$, which is quite close to the saturated value $C_1 = 1/12$ for the 2D homogeneous ferromagnet. Comparing figure 3 with figure 1, we also find that the quantum fluctuation close

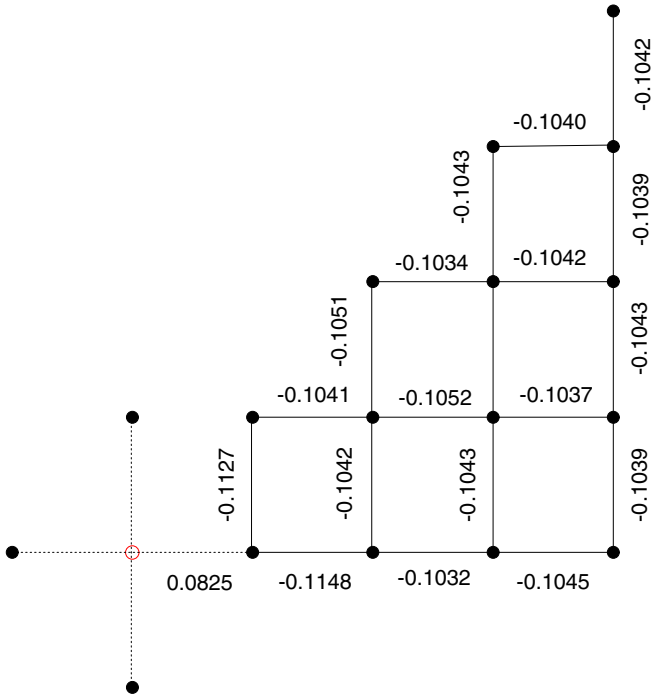

Figure 3. The nearest-neighbour correlation functions for the 8×8 lattice with one ferromagnetic impurity at temperature $T/J = 0.05$. The open circle represents the ferromagnetic impurity.

to the ferromagnetic impurity is weaker than that of the nonmagnetic impurity case.

We have also performed quantum Monte Carlo simulations for this system, using the numerically exact stochastic series expansion algorithm with a recently introduced global updating scheme [19]. Table 1 lists simulation results for lattices with 4×4, 8×8, and 16×16 spins, for two values of J_F at temperature $T/J = 0.05$. This temperature is sufficiently low to give the ground-state values of the short-range correlation functions. We also list results obtained with the Green's function approach. The Monte Carlo data show that finite-size effects are minor for both $C(1)$ and $C(2)$. The Green's function results for $C(2)$ agree very well with the QMC data. For $C(1)$ at $J_F/J = 1.0$, there is an approximately 10% discrepancy, and an even larger discrepancy at $J_F/J = 0.5$. Such discrepancies most likely arose from the decoupling scheme, equation (7), that we introduced. That approximation is good for the majority of antiferromagnetic coupled spin pairs but it is a poor approximation for the one ferromagnetic coupled bond which acts like a 'stranger to the family'.

Table 1. Comparison of SOGF and QMC results for spin–spin correlation functions for two values of J_F.

		$J_F/J = 1$		$J_F/J = 0.5$	
Method	Size	$C(1)$	$C(2)$	$C(1)$	$C(2)$
QMC	4×4	0.07528(3)	−0.11810(2)	0.06930(2)	−0.11965(2)
QMC	8×8	0.07411(6)	−0.11459(6)	0.07027(3)	−0.11530(3)
QMC	16×16	0.07375(3)	−0.11409(3)	0.07032(2)	−0.11477(3)
SOGF	8×8	0.0825	−0.1148	0.0515	−0.1150

Next we study the temperature dependence of the spin correlation functions $C(1)$ and $C(2)$ and the effect of the relative strength J_F/J in the range $J_F/J = [0, 1]$. Results for $C(1)$ and $C(2)$ calculated on an 8×8 lattice are plotted in figure 4. Squares show the results from quantum Monte Carlo simulations while circles show the results from the second-order Green's function approach. Figure 4(a) shows the temperature dependence of these correlation functions for $J_F/J = 1.0$ and 0.5. As expected, the quantum fluctuation close to the impurity decreases as temperatures increases. Figure 4(b) shows the dependence on the relative strength J_F/J at temperatures $T/J = 0.25$ and 1.0. The ferromagnetic correlation function $C(1)$ increases with J_F/J; that is, the quantum fluctuation closer to the impurity decreases as J_F/J increases. Figures 4(c) and 4(d) show results for $C(2)$. The agreement between the SOGF and QMC results is usually better for $C(2)$ than $C(1)$.

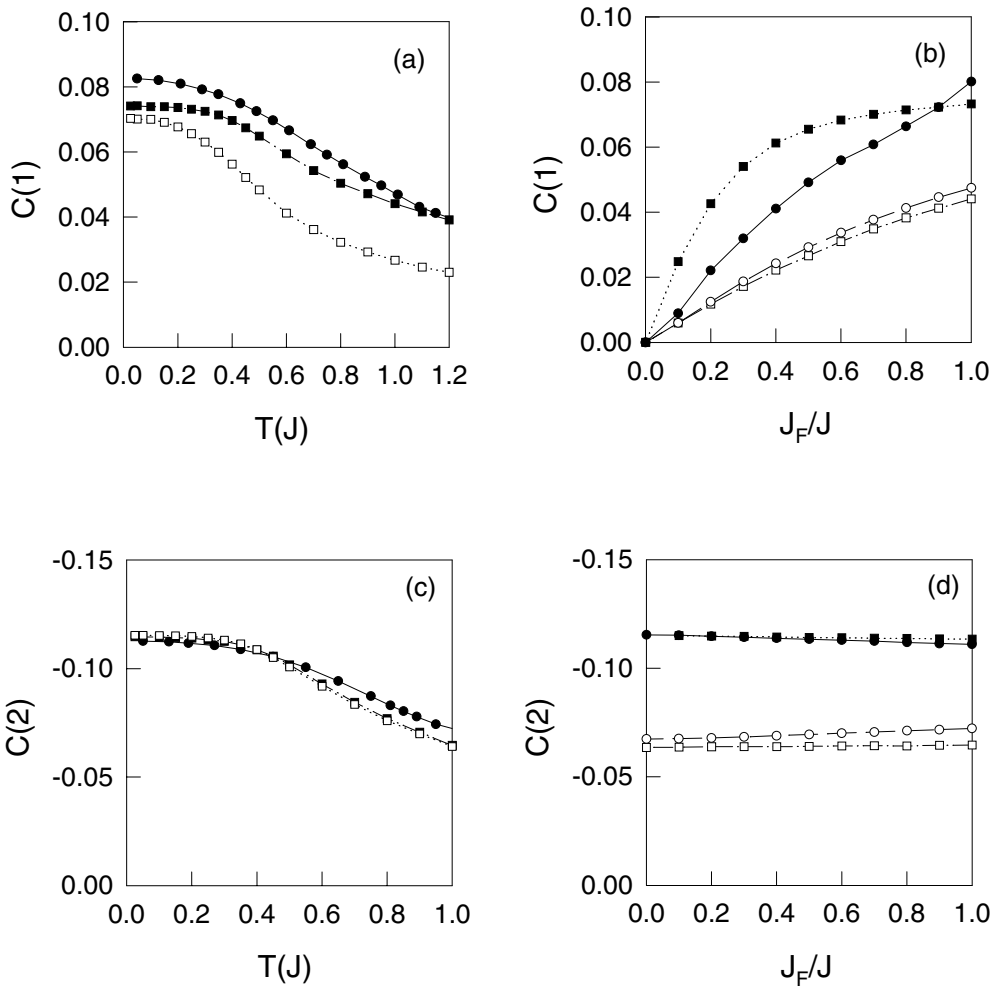

Figure 4. The spin correlation function on the ferromagnetic bond, $C(1)$, as a function of: (a) temperature for $J_F/J = 1.00$ (filled symbols) and 0.50 (open symbols); (b) the relative strength J_F/J at temperature $T/J = 0.25$ (filled symbols) and 1.00 (open symbols); and on the bond next to the ferromagnetic bond, $C(2)$: (c) as (a) but for $C(2)$; (d) as (b) but for $C(2)$. Squares show results from quantum Monte Carlo simulations while circles show results from the second-order Green's function approach. The results shown were calculated on an 8×8 lattice.

The spin-wave theory predicts that the behaviour of a spin-1/2 AF Heisenberg model on a square lattice is controlled by the continuous spin-wave excitations around a state characterized by LRO [20]. The continuous spin-wave excitations have been observed in the undoped material La_2CuO_4 in neutron scattering [28] and Raman scattering [29] experiments. Our improved SOGF theory also shows that, in the homogeneous case, there are continuous spin-wave excitations ranged from zero to $\omega = 4.73J$. After ferromagnetic impurities have been added into an AF system, the ferromagnetic defects tend to align the background spins in some range. That is, the local spin-wave excitations can form around the ferromagnetic impurities in the AF system, and the corresponding energy of the local spin-wave excitation is higher than those of the continuous spin-wave excitations. In addition, there is a discrete energy level above the continuous spin-wave spectrum. The local spin-wave excitation is also called the local mode. Since the energy of the local mode is much higher than that of the continuous spin-wave excitations, it has little effect on the thermodynamic properties of the magnetic system, while in the neutron scattering experiment, the energy of neutrons is high enough to excite the local spin-wave excitation. It is expected that some new peaks will be observed in the neuron scattering experiment. These peaks correspond to the local modes.

In the ferromagnetic impurity case, our SOGF calculations also show that there are discrete local modes emerging above the continuous spin-wave excitations. In contrast, we found no local mode in the nonmagnetic impurity case. These local modes are excited by the local spin excitation around the ferromagnetic impurities (see below). For a system with one ferromagnetic impurity, we found that there is only one corresponding local mode above the continuous spin-wave excitations. In figure 5, we plot the temperature dependence of the excitation energy of the local mode (filled circles) and the band top of the continuous spin-wave

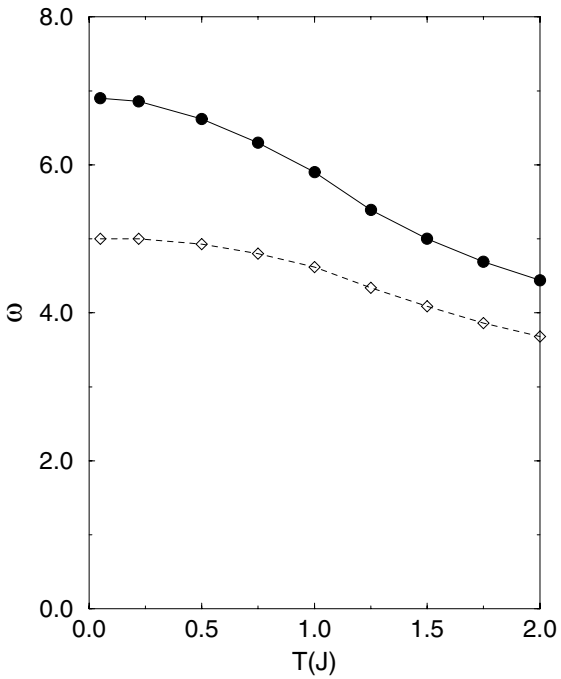

Figure 5. The temperature dependence of the excitation energy of the local mode (filled circles) and the band top of the spin-wave spectrum (open diamonds) in the one-ferromagnetic-impurity case.

excitations (diamonds). The excitation energy of the local mode decreases as temperature increases. In the ground state, the energy gap between the local mode and the band top of the spin-wave excitations is $\Delta = 1.90$. This gap decreases as the temperature increases. Our results show that the local excitation around the ferromagnetic impurity is reduced as temperature increases.

For a system with two ferromagnetic impurities, we found two corresponding local modes. The excitation energy of these two local modes depends strongly on the relative position of the two ferromagnetic impurities. That is, there is strong interaction among the local spin excitations around these two ferromagnetic impurities. In our calculation, we found that the AF Heisenberg system with two ferromagnetic impurities can be divided into two types, which are shown in figure 6. It can be seen from figure 6(a) that the two ferromagnetic impurities are on the same sublattice and they compose an effective triplet state (ETS), while in figure 6(b) the two impurities are on the two different sublattices and they form an effective singlet state (ESS). The distance dependences of the excitation energies of these two local modes for the ETS and the ESS at temperature $T/J = 0.05$ are plotted in figures 7(a) and 7(b), respectively. In figure 7(a), we found that there is a large energy gap between the two local modes of the ETS as the two ferromagnetic impurities are very close. This gap decreases rapidly as the distance between these two impurities increases. This means that the strong interaction between the local spin excitations around the two ferromagnetic impurities drops quickly as the two ferromagnetic impurities draw apart from each other. However, in figure 7(b), the corresponding gap of the ESS is significantly smaller than that of the ETS. It is also clear that the excitation energy of these two local modes in the ESS is smaller than that of the ETS. Furthermore, we also found that the continuous spin-wave excitations for the AF background are strongly affected by the appearance of these local modes. The band top of the continuous

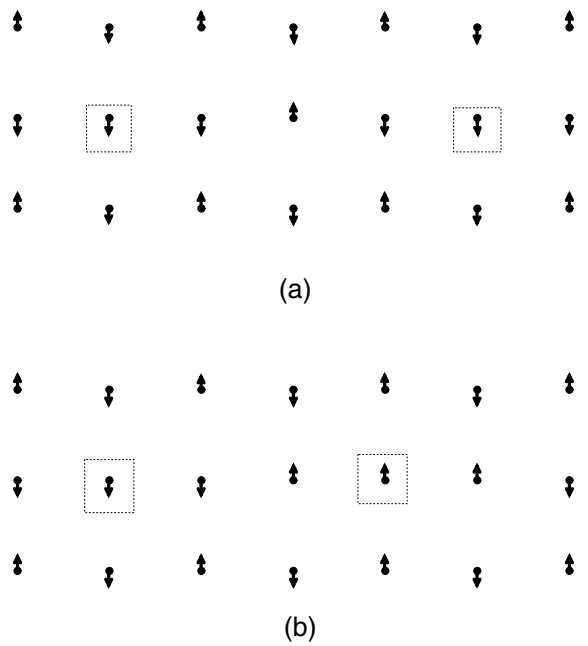

Figure 6. Two kinds of antiferromagnetic system with two ferromagnetic impurities: (a) the two impurities are in the same sublattice; (b) the two impurities are in different sublattices. Dashed squares represent the two ferromagnetic impurities.

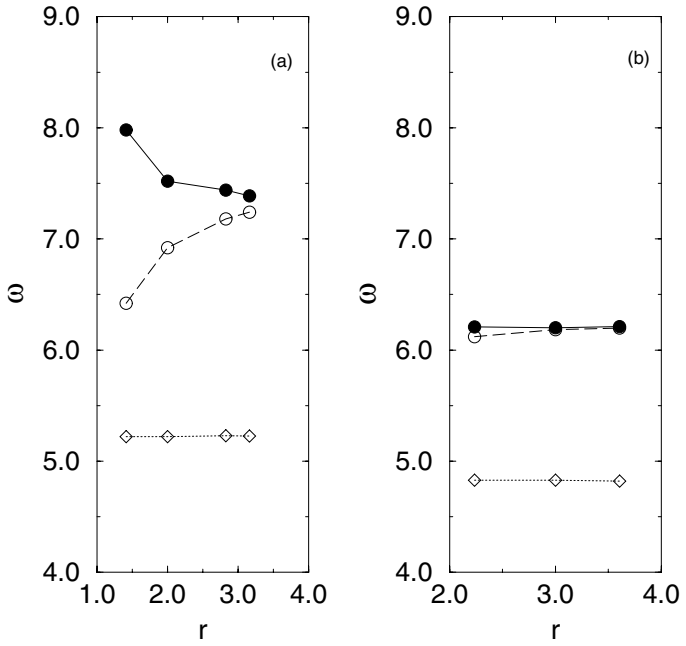

Figure 7. The distance dependence of the excitation energy of the two local modes (filled and open circles) and the band top of the spin-wave spectrum (open diamonds) in the two-ferromagnetic-impurity cases ETS (a) and ESS (b).

spin-wave excitations of the ETS is $E_{\text{top}} = 5.40J$, which is larger than that of the ESS ($E_{\text{top}} = 4.75J$), while for the one-impurity case, E_{top} is equal to $5.00J$. Thus we conclude that the two ferromagnetic impurities prefer to form an ESS. In both figures 7(a) and 7(b), E_{top} remains almost unchanged as the separation of these two impurities increases, which suggests that the continuous spin-wave excitation spectrum is a characteristic property for both the ESS and the ETS.

5. Summary

In conclusion, we have studied the 2D spin-1/2 Heisenberg model with nonmagnetic and ferromagnetic impurities by using the improved second-order Green's function theory and quantum Monte Carlo simulations. The second-order Green's function theory has been proved to be applicable to spin systems with spatial inhomogeneity. For both nonmagnetic and ferromagnetic impurity cases, results obtained from the Green's function theory agree with those from quantum Monte Carlo simulations. In our calculations, we found that the spatial distributions of the antiferromagnetic correlation functions close to the isolated impurities are enhanced in both the nonmagnetic and ferromagnetic cases. The quantum fluctuation close to the isolated ferromagnetic impurity is weaker than that close to the nonmagnetic impurity. For systems with ferromagnetic impurities, our results showed that there are local modes emerging above the continuous spin-wave excitations. Each ferromagnetic impurity can excite one corresponding local mode. When there are two ferromagnetic impurities in the system, we found strong interaction between the two local modes, and this interaction depends strongly on the relative position of the two ferromagnetic impurities. The antiferromagnetic systems with two local ferromagnetic impurities can be divided into two types, one with an

effective triplet state and the other one with an effective singlet state. Our numerical results showed that two ferromagnetic impurities prefer to form an effective singlet state.

Acknowledgments

We thank Professor Shiping Feng and Professor Jue-Lian Shen for helpful discussions. This work was supported in part by the Earmarked Grant for Research from the Research Grants Council (RGC) of the Hong Kong Government under Projects CUHK311/96P-2160068 and 4190/97P-2160089. AWS would like to thank the Department of Physics at the Chinese University of Hong Kong for hospitality and financial support during a visit. Support from the NSF under Grant No DMR-9712765 is also acknowledged.

References

[1] Kampf A P 1994 *Phys. Rep.* **249** 219
[2] Dagotto E 1994 *Rev. Mod. Phys.* **66** 763
[3] Xiao G, Cieplak M Z, Xiao J Q and Chien C L 1990 *Phys. Rev.* B **42** 8752
[4] Chakraborty A, Epstein A J, Jarrell M and McCurron E M 1989 *Phys. Rev.* B **40** 5296
[5] Keimer B, Belk N, Birgeneau R J, Cassanho A, Chen C Y, Greven M, Kastner M A, Aharony A, Endoh Y, Erwin R W and Shirane G 1992 *Phys. Rev.* B **46** 14 034
[6] Brening W and Kampf A P 1991 *Phys. Rev.* B **43** 12 914
[7] Bulut N, Hone D, Scalapino D J and Loh E Y 1989 *Phys. Rev. Lett.* **62** 2192
[8] Kawashima B and Oguchi A 1994 *J. Phys. Soc. Japan* **63** 1908
[9] Acquarone M and Paiusco M 1993 *Physica* C **210** 373
[10] Nonomura Y 1996 *J. Phys. Soc. Japan* **65** 402
[11] Manousakis E 1992 *Phys. Rev.* B **45** 7570
[12] Behre J and Miyashita S 1992 *J. Phys. A: Math. Gen.* **25** 4745
[13] Sandvik A W, Dagotto E and Scalapino D J 1997 *Phys. Rev.* B **56** 11 701
[14] Mermin N D and Wagner H 1966 *Phys. Rev. Lett.* **22** 1133
[15] Manousakis E 1991 *Rev. Mod. Phys.* **63** 1
[16] Neves E J and Peres J F 1986 *Phys. Lett.* A **114** 331
Dyson F J, Lieb E H and Simon B 1987 *J. Stat. Phys.* **18** 335
Affleck I, Kennedy T, Lieb E H and Tasaki H 1988 *Commun. Math. Phys.* **155** 477
[17] Kondo J and Yamaji K 1972 *Prog. Theor. Phys.* **47** 807
[18] Shimahara H and Takada S 1991 *J. Phys. Soc. Japan* **60** 2394
[19] Sandvik A W 1997 *Phys. Rev.* B **56** 11 678
Sandvik A W 1999 *Phys. Rev.* B **59** R14156
(Sandvik A W 1999 *Preprint* cond-mat/9902226)
[20] Anderson P W 1952 *Phys. Rev.* **86** 694
[21] Rushbrooke G S, Baker G A and Wood P J 1974 *Phase Transitions and Critical Phenomena* (New York: Academic)
[22] Takahashi M 1989 *Phys. Rev.* B **40** 2494
[23] Bonner J C and Fisher M E 1964 *Phys. Rev.* **135** A640
[24] Okabe Y and Kikuchi M 1988 *J. Phys. Soc. Japan* **57** 4351
[25] Zhang W J, Shen J L, Xu J H and Ting C S 1995 *Phys. Rev.* B **51** 2950
[26] Fukumoto Y and Oguchi A 1996 *J. Phys. Soc. Japan* **65** 264
[27] Song Yun, Lin H Q and Shen Jue-Lian 1998 *Phys. Rev.* B **58** 9166
[28] Aeppli G, Hayden S M, Mook H A, Fisk Z, Cheong S-W, Rytz D, Remeika J P, Espinosa G P and Cooper A S 1989 *Phys. Rev. Lett.* **62** 2052
[29] Lyons K B, Sulewski P E, Fleury P A, Carter H L, Cooper A S, Espinosa G P, Fisk Z and Cheong S-W 1989 *Phys. Rev.* B **38** 9693